Electronic Supplementary Information

Water-Induced Helical Supramolecular Polymerization and Gel Formation of Alkylene-Tethered Perylene Bisimide Dyad

Xu Lin,[a] Hiroki Kurata,[a] Deepak D. Prabhu,[a] Mitsuaki Yamauchi,[a] Tomonori Ohba[b] and Shiki Yagai*[a]

[a] Department of Applied Chemistry and Biotechnology, Graduate School of Engineering, Chiba University, 1-33 Yayoi-cho, Inage-ku, Chiba 263-8522, Japan.
[b] Department of Chemistry, Graduate School of Science, Chiba University, 1-33 Yayoi-cho, Inage-ku, Chiba 263-8522, Japan.

Table of Contents

1. Materials and Methods

All commercially available reagents and solvents were of reagent grade and used without further purification. NMR spectra were recorded on JEOL JNM-ECA500 NMR spectrometers and chemical shifts are reported in ppm (δ) with the signal of TMS as an internal standard. ESI-MS spectra were measured on an Exactive (Thermo Scientific). UV/Vis and fluorescence spectra were recorded on a JASCO V660 spectrophotometer and JASCO FP6600 spectrofluorometer, respectively. Fluorescence quantum yields were measured on Absolute PL Quantum Yield Measurement System C9920-02 (Hamamatsu Photonics). Circular dichroism (CD) and linear dichroism (LD) spectra were recorded on a JASCO J840 spectropolarimeter equipped. Powder X-ray diffraction analysis was carried out with a Rigaku Rint-2200 X-ray diffractometer with monochromated CuKα radiation ($\lambda = 1.5418$ Å). All X-ray diffraction experiments were performed at room temperature. TEM observation was performed on JEM-2100F (JEOL) at acceleration voltage at 120 kV. The sample was prepared by spin-coating assembly solution onto carbon-coated formvar copper grid (200 mesh) and dried under vacuum for 24 h. AFM images were acquired under ambient conditions using Multimode 8 Nanoscope V (Bruker Instruments) in tapping mode. Silicon cantilevers (OMCL-AC240TS-C2) with a spring constant of 2 N/m and frequency of 70 kHz (nominal value, S2 Olympus, Japan) were used. The samples were prepared by spin-coating solution onto freshly cleaved highly-oriented pyrolytic graphite (HOPG). Rheological measurements were performed using the parallel plate geometry (DICOVERY HR-3, TA Instruments, USA) at 25 °C.

2. Synthesis and characterization

Perylene bisimide dyad **2** was prepared according to Scheme S1. Compounds **3**[S1], **4**[S2] and **5**[S3] were prepared according to reported methods.

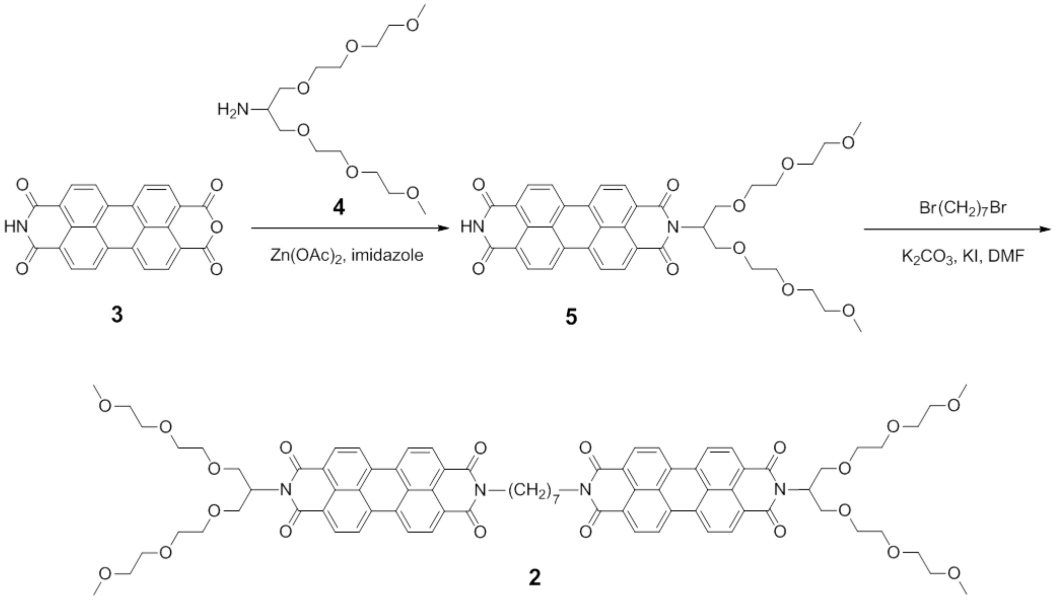

Scheme S1. Synthesis of perylene bisimide dyad **2**

A mixture of **5** (200 mg, 0.30 mmol), 1,7-dibromoheptane (41 mg, 0.15 mmol), K_2CO_3 (74 mg, 0.54 mmol) and KI (10 mg, 0.06 mmol) in DMF (15 mL) was stirred for 5 h at 80 °C under N_2 atmosphere. After the solution was cooled to room temperature, the solvent was removed under vacuum. The residue was purified by silica gel column chromatography (eluent: 5% methanol in chloroform) and GPC (eluent: chloroform) to give pure compound **2** as a red solid (61 mg, 28%). ^{1}H NMR (500 MHz, $CDCl_3$) δ = 8.33 (d, J = 7.9 Hz, 4H, Ar*H*), 8.25 (d, J = 7.4 Hz, 4H, Ar*H*), 8.05− 8.00 (m, 8*H*, Ar*H*), 5.68−5.60 (m, 2*H*, 2N−C*H*-OEG), 4.23−4.15 (m, 8*H*, 2N−CH_2 and 2αOCH_2−OEG), 4.00 (dd, 4*H*, 2αOCH_2−OEG), 3.79−3.57 (m, 24*H*, 12OCH_2−OEG), 3.46−3.44 (m, 8*H*, 4OCH_2−OEG), 3.30 (s, 12*H*, 4OCH_3−OEG), 1.87−1.78 (m, 4*H*, 2CH_2), 1.58−1.49 (m, 6*H*, 3CH_2) ppm; ^{13}C NMR (125 MHz, $CDCl_3$, 60 °C) δ = 163.18, 162.74, 133.41, 133.27, 130.60, 130.53, 128.77, 128.59, 125.32, 125.21, 123.11, 122.91, 122.21, 122.17, 72.05, 70.65, 70.53, 70.48, 69.51, 58.89, 52.58, 40.60, 29.85, 28.13, 26.57 ppm; HRMS (ESI): m/z calcd for $C_{81}H_{84}N_4O_{20}Na$

1455.5571 [M+Na]$^+$, found 1455.5564.

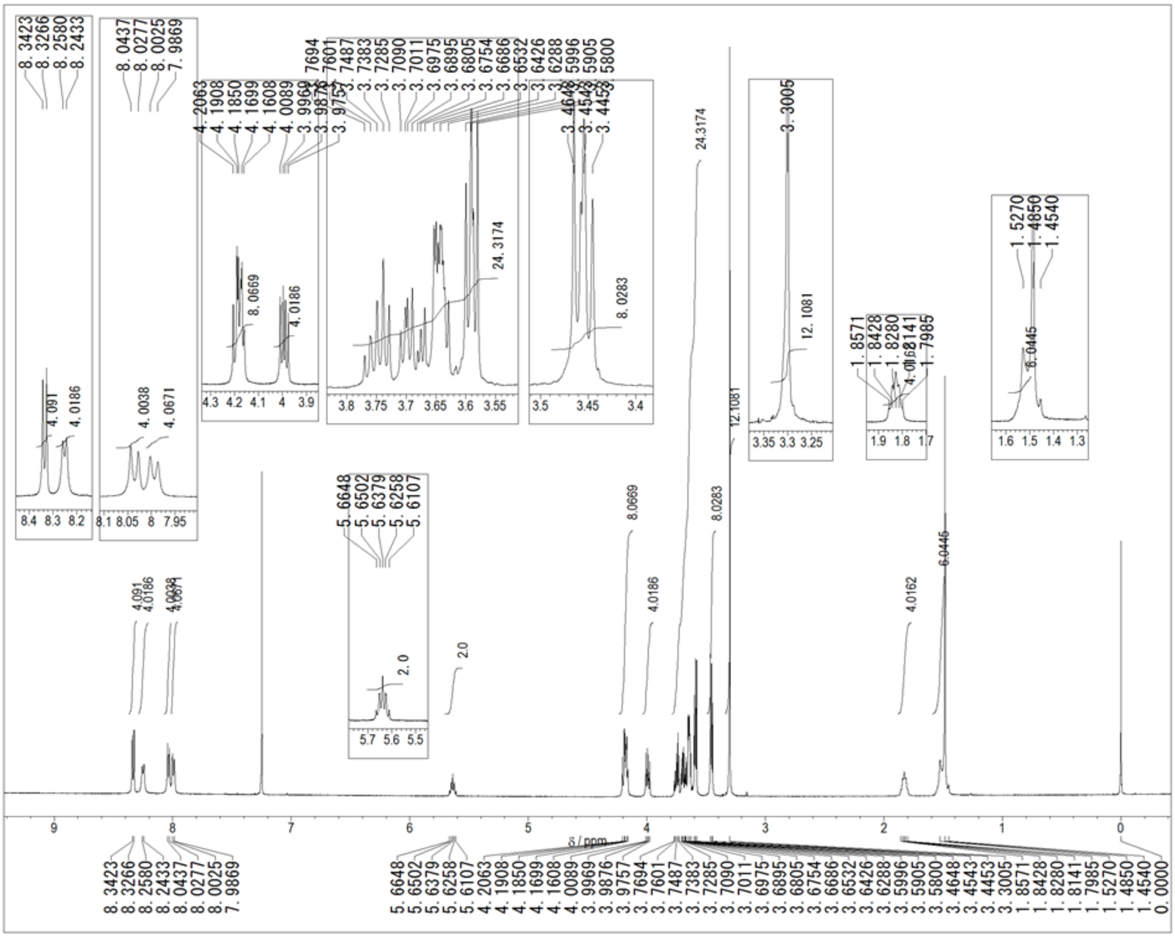

Chart S1 ^{1}H NMR spectrum of **2** in CDCl$_3$ at 293 K.

3. Supporting Figures

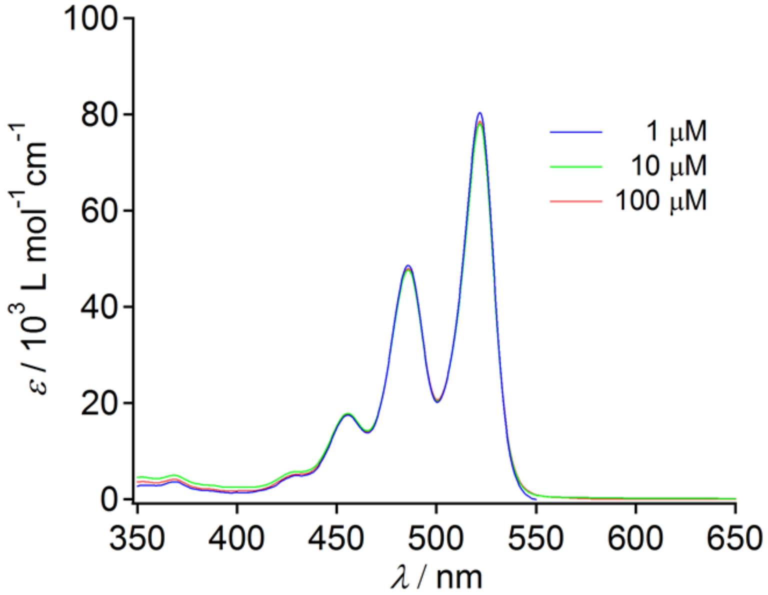

Fig. S1 Concentration-dependent UV/Vis absorption spectra of **1** ($c = 1 \times 10^{-6}$ to 1×10^{-4} M) in THF at 20 °C.

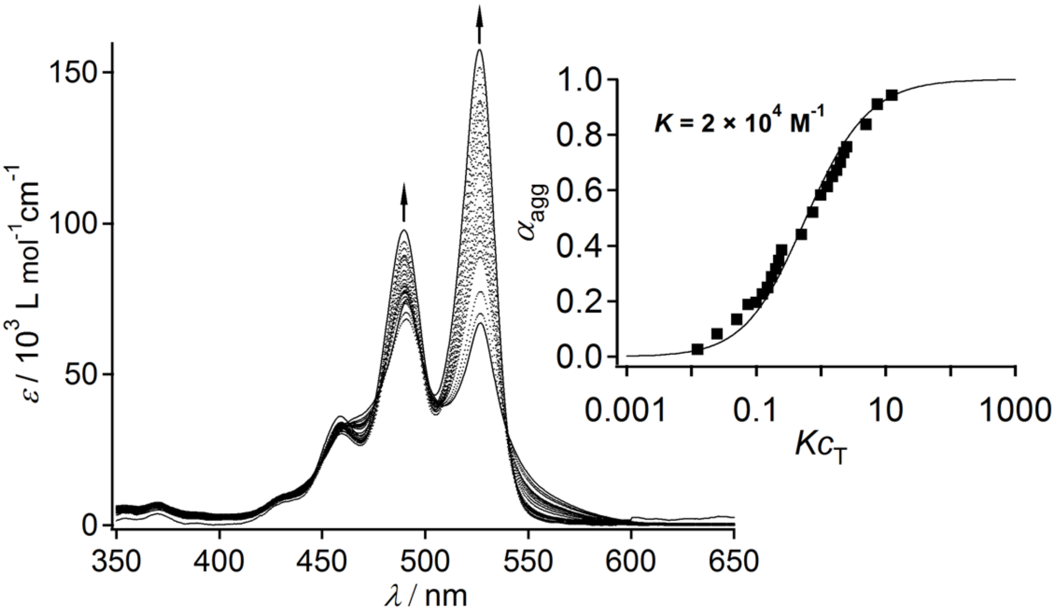

Fig. S2 Concentration-dependent UV/Vis absorption spectra of **2** ($c = 5 \times 10^{-7}$ to 1×10^{-3} M) in $CHCl_3$/THF (8/2, v/v) mixture at 20 °C. Arrows indicate spectral change with decreasing concentration. Inset: plot of fraction of aggregated molecules (α_{agg}) of **2** calculated from apparent absorption intensity at $\lambda = 522$ nm as a function of Kc_T. The solid line corresponds to the theoretical fit obtained by using isodesmic model. K denotes the association constant.

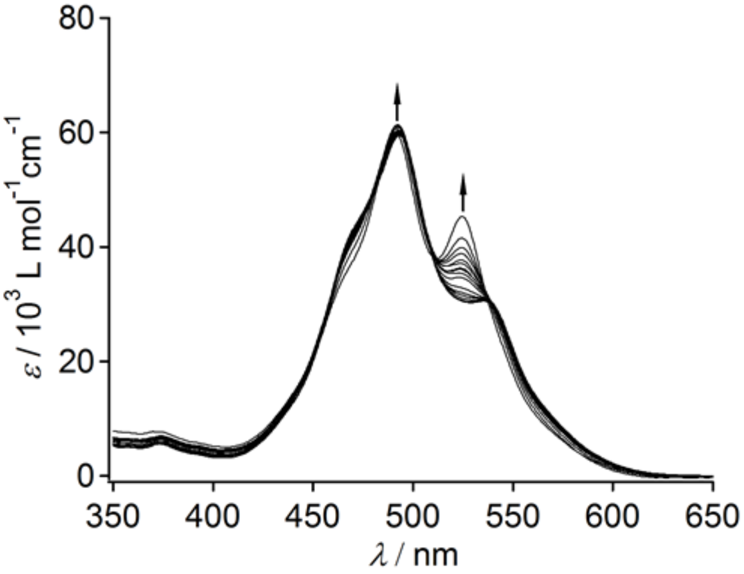

Fig. S3 Concentration-dependent UV/Vis absorption spectra of **2** ($c = 1 \times 10^{-6}$ to 1×10^{-4} M) in THF/water mixtures (80/20) at 20 °C. Arrows indicate the spectral changes with decreasing concentration.

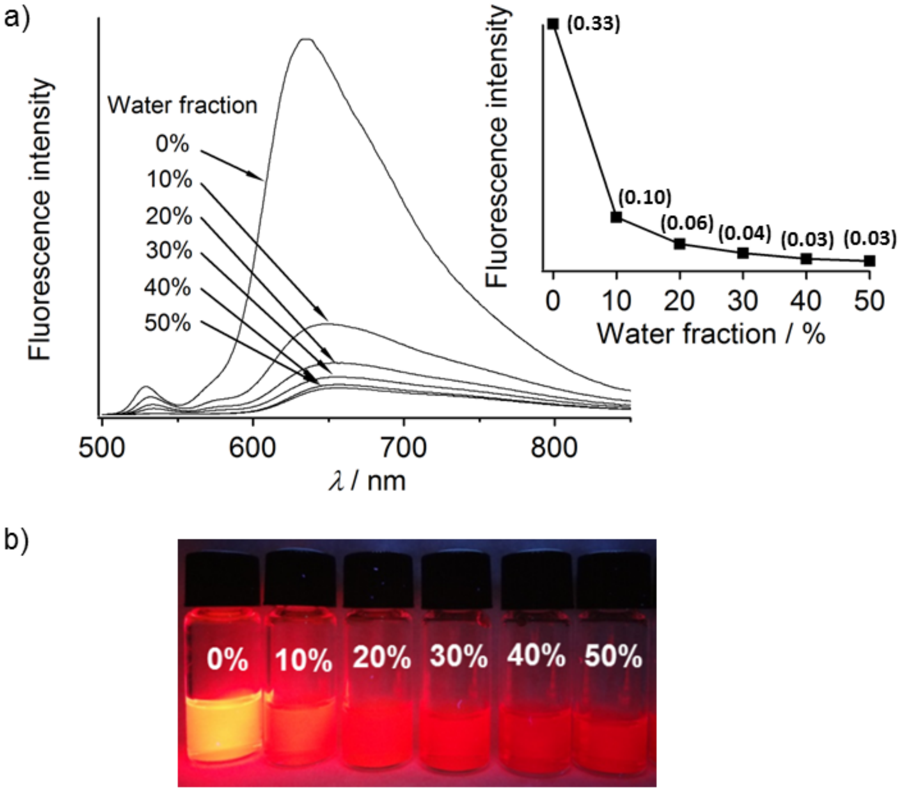

Fig. S4 a) Fluorescence spectra of **2** ($c = 1 \times 10^{-4}$ M, $\lambda_{ex} = 470$ nm) in THF/water mixtures with different water content (0–50 v/v%). Inset: plots of the intensity of excimer-like fluorescence (λ_{max}) as a function of different water content. Numbers in parentheses indicate the fluorescence quantum yield (Φ_f) of **2**. b) Photographs of dyad **2** ($c = 1 \times 10^{-4}$ M) in THF/water mixture with different water content (0−50, v/v%) under UV-illumination.

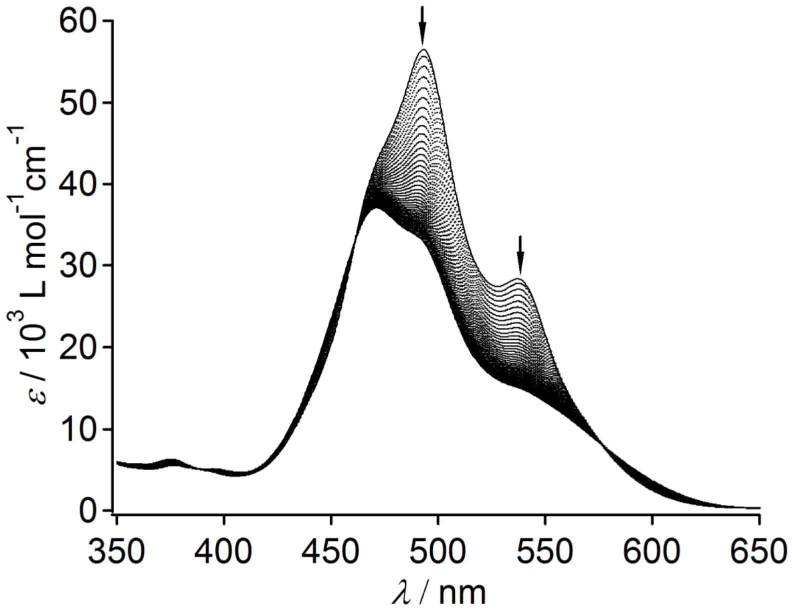

Fig. S5 Time-dependent UV/Vis absorption spectra of **2** (c = 1 × 10^{-4} M) in THF/water (60/40) mixture at 20 °C (1–300 min). Arrows indicate the spectral changes with time.

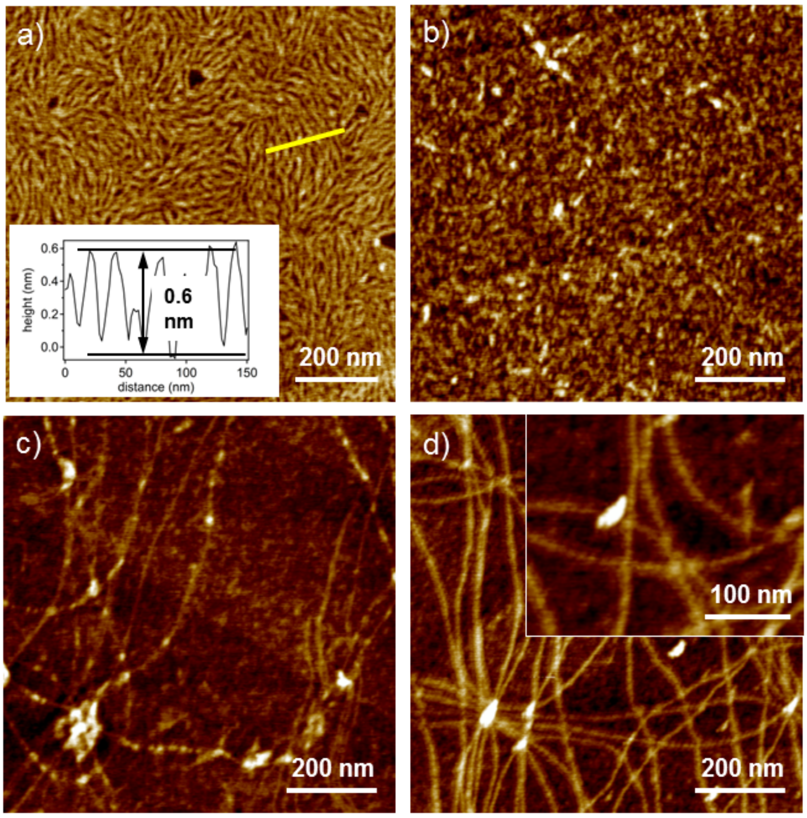

Fig. S6 a) AFM height image of **2** spin-coated from THF solution (c = 1 × 10^{-4} M) onto highly oriented pyrolytic graphite (HOPG). Inset: cross-sectional analysis along yellow line in a). b-d) AFM height images of **2** (c = 1 × 10^{-4} M) spin-coated from THF/water (50/50) mixture after an equilibration time of b) 1 min, c) 5 min and d) 15 min.

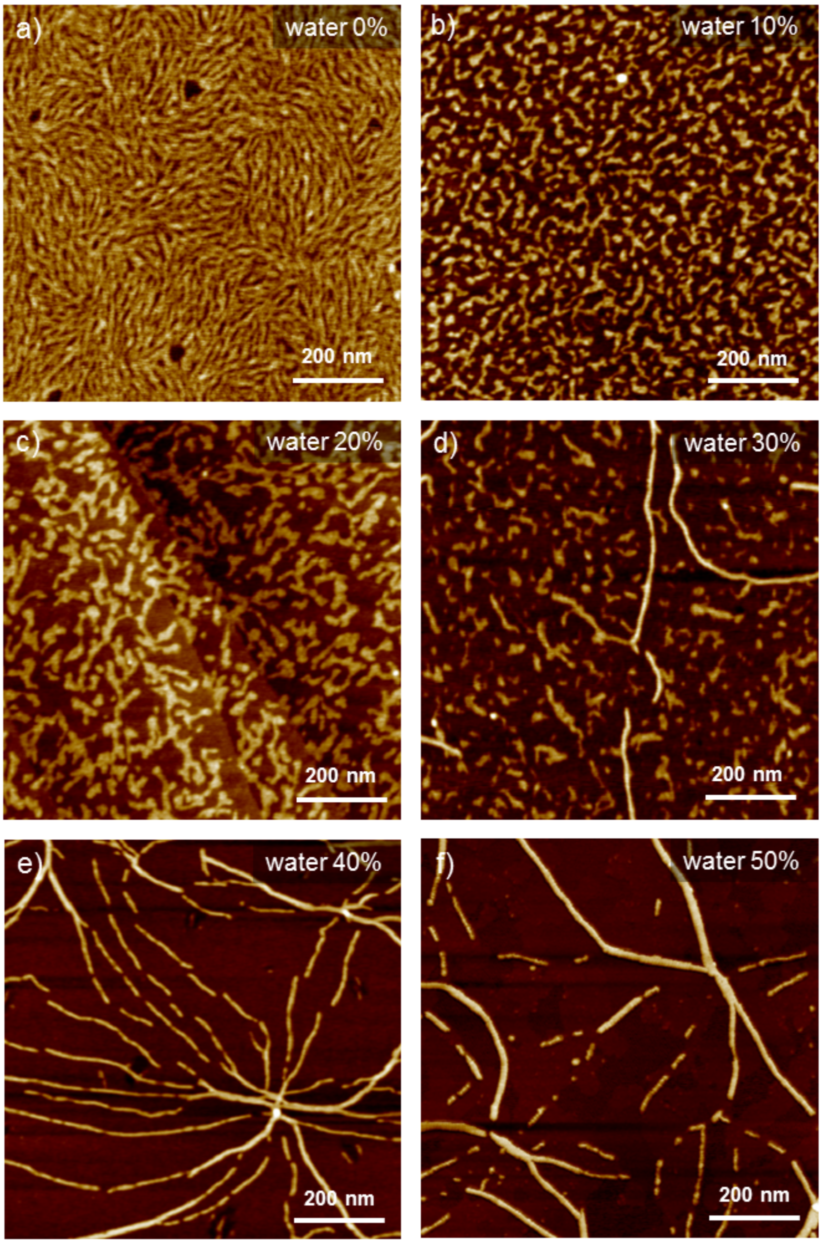

Fig. S7 AFM height images of aggregated **2** ($c = 1 \times 10^{-4}$ M) spin-coated from different THF/water mixtures onto HOPG. Water content: a) 0%, b) 10%, c) 20%, d) 30%, e) 40%, and f) 50%. The AFM imaging was carried out after 6 h of incubation.

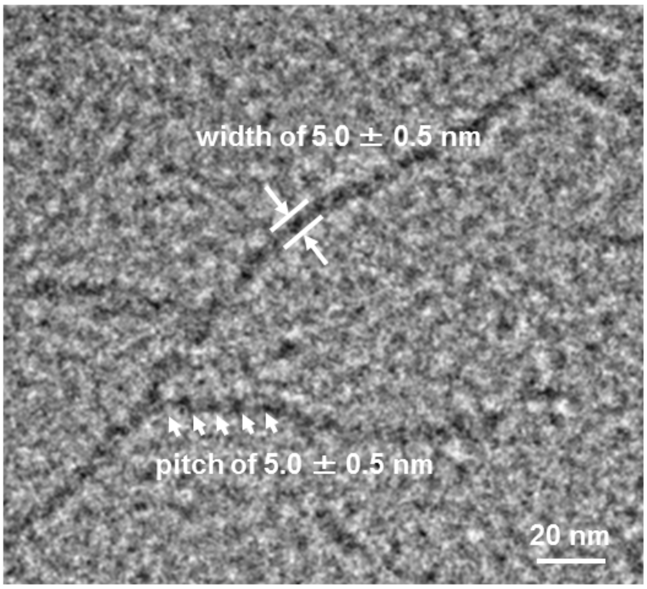

Fig. S8 TEM image of helical supramolecular polymers of **2** formed in THF/water (50/50) mixture ($c = 1 \times 10^{-4}$ M). The sample was prepared by spin-coating the solution onto carbon-coated formvar copper grid (200 mesh).

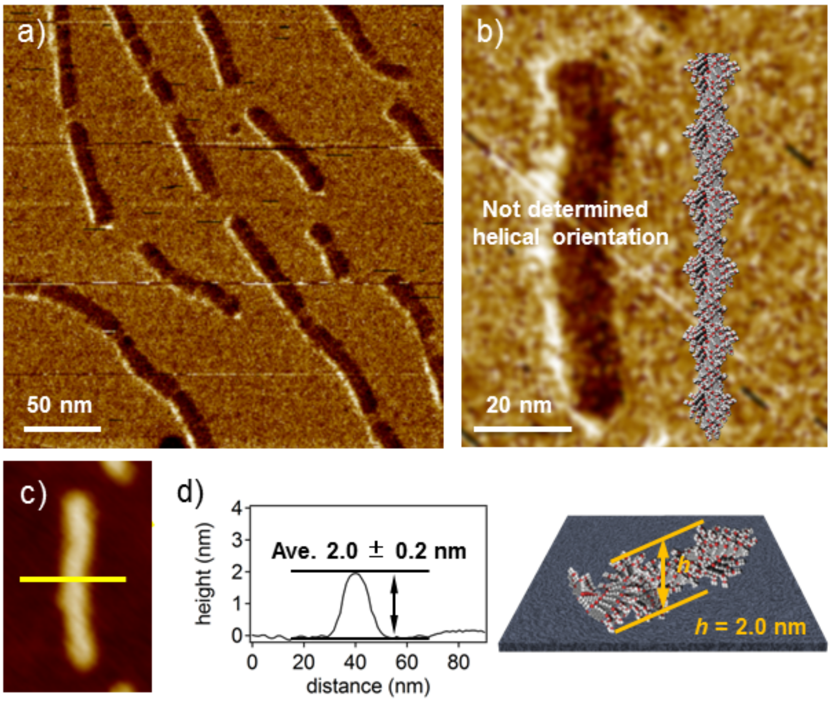

Fig. S9 a) AFM phase image of **2** ($c = 1 \times 10^{-4}$ M) spin-coated from THF/water (40/60) onto HOPG. b) Magnified image of a fiber with proposed aggregate structure. c) AFM height image of the fiber. d) Cross-sectional analysis along the yellow line in c) with schematic representation of the fiber on the substrate.

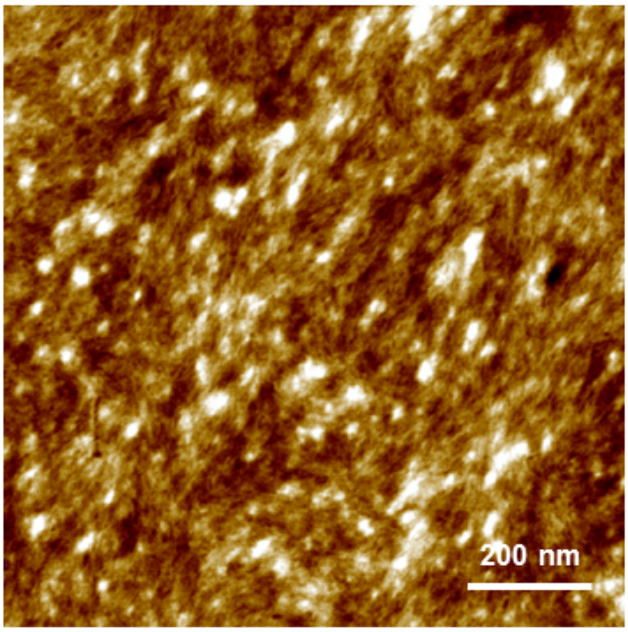

Fig. S10 AFM height image of the precipitate formed in the supersaturated THF solution of **2** ($c = 2 \times 10^{-4}$ M) spin-coated onto HOPG.

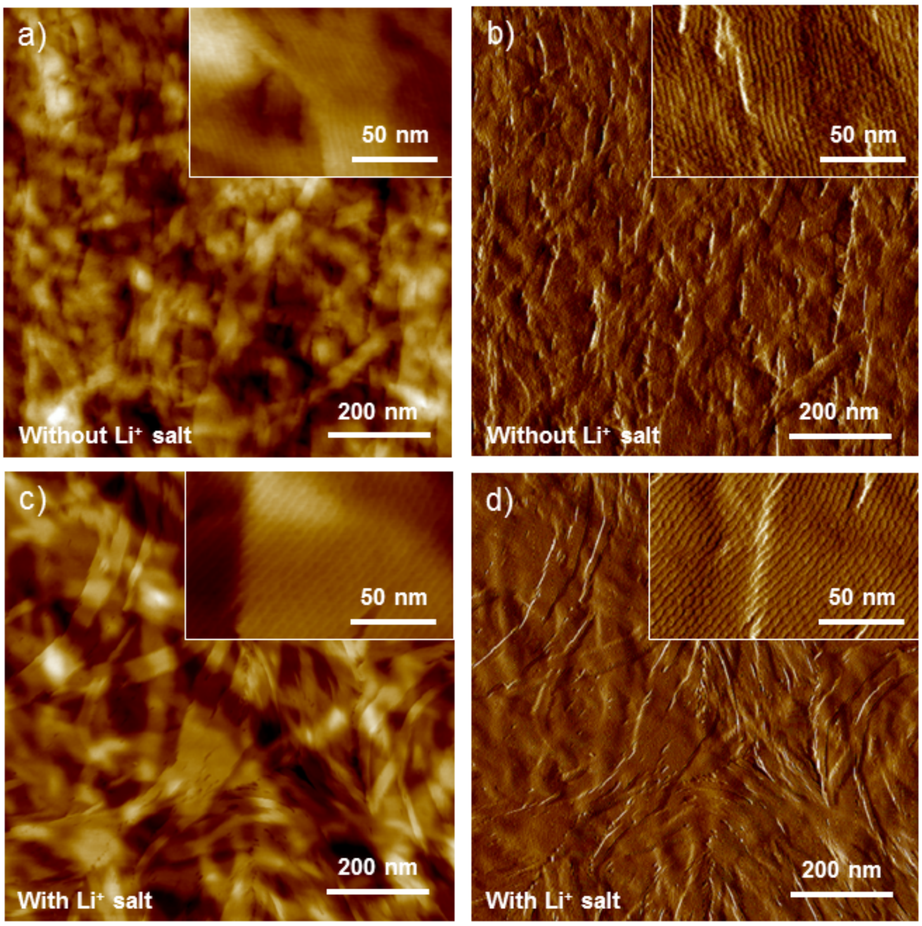

Fig. S11 AFM a,c) height and b,d) error images of xerogels of **2** ($c = 1.0 \times 10^{-3}$ M) a,b) without Li^+ salt and c,d) with Li^+ salt.

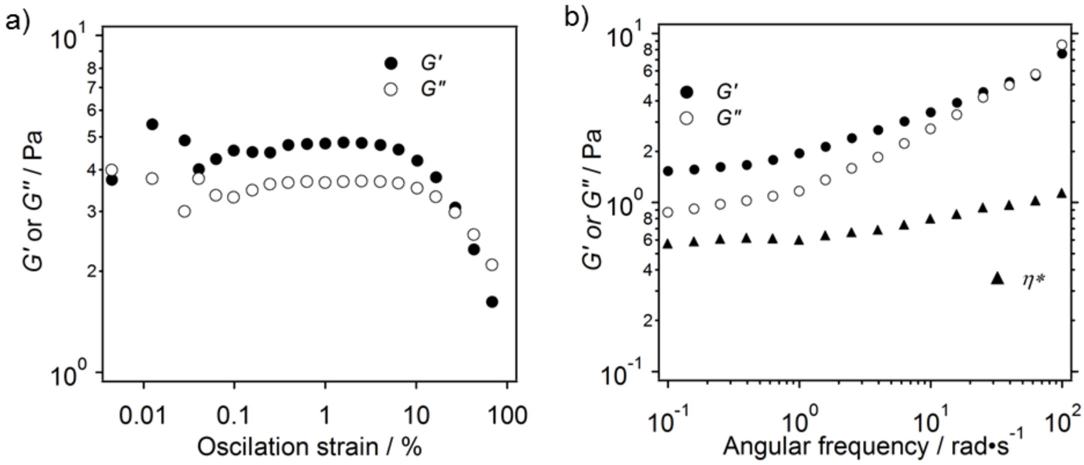

Fig. S12 a) Dynamic moduli, storage modulus (G') and loss modulus (G''), versus oscillation strain for a gel of **2** ($c = 3.0 \times 10^{-3}$ M) in THF/ water (50/50) mixture. The data were acquired at 25 °C. b) Dynamic moduli, storage modulus (G'), loss modulus (G''), and complex viscosity (η^*) versus angular frequency for a gel of **2** ($c = 3.0 \times 10^{-3}$ M) in THF/water (50/50) mixture at 25 °C. Strain amplitude: 10%.

Table S1 *d*-Spacing values and lattice parameters of dried gel of **2.**

Assigned	*d*-spacing / Å	(hkl)	lattice parameters / Å
Col$_h$	25.5	(100)	*a* = 29.9
	14.9	(110)	
	13.0	(200)	
	9.4	(210)	
	7.3	(220)	

The *d*-spacing ratio was found to be $1:\frac{1}{\sqrt{3}}:\frac{1}{2}:\frac{1}{\sqrt{7}}:\frac{1}{3}:\frac{1}{\sqrt{12}}$ indicating a hexagonal columnar arrangement.

4. Supporting References

S1 N. Pasaogullari, H. Icil and M. Demuth, *Dyes and Pigments,* 2006, **69**, 118–127.

S2 R. Samudrala, X. Zhang, R. M. Wadkins and D. L. Mattern, *Bioorg. Med. Chem.,* 2007, **15**, 186–193.

S3 A. Wicklein, A. Lang, M. Muth and M. Thelakkat, *J. Am. Chem. Soc.,* 2009, **131**, 14442–14453.